[CANCER RESEARCH 63, 1000–1011, March 1, 2003]

Apoptotic Susceptibility of Cancer Cells Selected for Camptothecin Resistance: Gene Expression Profiling, Functional Analysis, and Molecular Interaction Mapping

William C. Reinhold,[1] Hosein Kouros-Mehr,[2] Kurt W. Kohn, Alika K. Maunakea, Samir Lababidi, Anna Roschke, Kristen Stover, Jes Alexander, Panayotis Pantazis, Lance Miller,[3] Edison Liu,[3] Ilan R. Kirsch, Yoshimasa Urasaki, Yves Pommier, and John N. Weinstein[1]

Laboratory of Molecular Pharmacology [W. C. R., H. K-M., K. W. K., A. K. M., S. L., J. A., Y. U., Y. P., J. N. W.] and Genetics Branch [A. R., K. S., I. R. K.], Center for Cancer Research, National Cancer Institute, NIH, Bethesda, Maryland 20892; University of Miami, Coral Gables, Florida 33146 [P. P.]; Advanced Technology Center, National Cancer Institute, Gaithersburg, Maryland 20874 [L. M., E. L.]; and First Department of Internal Medicine, Fukui Medical University, Fukui 910-1193, Japan [Y. U.]

ABSTRACT

To study the molecular mechanisms by which drug resistance develops, we compared DU145 human prostate cancer cells with a subline selected for resistance to camptothecin. Differences in gene expression level were assessed by hybridizing the two cell types against each other using quadruplicate "Oncochip" cDNA microarrays that included 1648 cancer-related genes. Expression levels differing by a factor of >1.5 were detected for 181 of the genes. These differences were judged statistically reliable on the basis of a stratum-adjusted Kruskal-Wallis test, after taking into account a dye-dependent variable. The 181 expression-altered genes included a larger than expected number of the "apoptosis-related" genes ($P = 0.04$). To assess whether this observation reflected a generalized resistance of RCO.1 to apoptosis, we exposed the cells to a range of stresses (cisplatin, staurosporine, UV, ionizing radiation, and serum starvation) and found greatly reduced apoptotic responses for RC0.1 (relative to DU145) using flow cytometric Annexin V and terminal deoxynucleotidyl transferase-mediated nick end labeling assays. We next examined the apoptosis-related genes in the context of a molecular interaction map and found expression differences in the direction "expected" on the basis of the apoptosis-resistance of RC0.1 for BAD, caspase-6, and genes that signal via the Akt pathway. Exposure of the cells to wortmannin, an inhibitor of the Akt effector phosphatidylinositol 3-kinase, provided functional support for involvement of the Akt pathway. However, closer examination of the molecular interaction map revealed a paradox: many of the expression differences observed for apoptosis-related genes were in the direction "contrary" to that expected given the resistance of RC0.1. The map indicated that most of these unexpected expression differences were associated with genes involved in the nuclear factor κB and transforming growth factor β pathways. Overall, the patterns that emerged suggested a two-step model for the selection process that led to resistance in RC0.1 cells. The first hypothesized step would involve a decrease in apoptotic susceptibility through changes in the apoptosis-control machinery associated with the Bcl-2 and caspase gene families, and also in antiapoptotic pathways operating through Akt/PKB. The second step would involve changes in multifunctional upstream genes (including some genes in the nuclear factor κB and transforming growth factor β pathways) that can facilitate apoptosis but that would also tend to contribute to cell proliferation in the presence of drug. Thus, we propose that a downstream blockade of apoptosis was "permissive" for the selection of upstream pathway changes that would otherwise have induced apoptosis. This model is analogous to one suggested previously for the relationship between oncogene function and apoptosis in carcinogenesis.

INTRODUCTION

Acquired resistance to multiple forms of treatment seriously limits the efficacy of cancer chemotherapy. One drug affected by acquired resistance is camptothecin, which poisons top1[4] by reversibly stabilizing DNA-top1 cleavable complexes (1–3). Camptothecin analogues are used clinically against multiple forms of cancer, including lung, breast, ovarian, and colorectal, but one factor that limits their activity is drug resistance, either primary or else secondary to treatment. Top1 mutations can explain resistance in some experimental models (1, 4), but they have not been implicated in clinical resistance to camptothecins. Hence, it seems likely that molecular alterations downstream from the top1 cleavable complexes are involved. To investigate that possibility in the present study we compared the prostate cancer cell line DU145 with a selected resistant subline RC0.1 (5). It is worth noting that such a study could not have been done with transfected or knockout cells insofar as multiple gene changes are involved (6).

DU145 is an androgen-independent, mismatch repair-deficient (7), microsatellite-unstable (8) human cell line derived from metastatic disease (9, 10). In their late stages, clinically metastatic and androgen-independent prostatic cancers tend to be aggressive and are uniformly fatal. 9-Nitro-camptothecin has been shown to activate a CD95 (Fas)/CD95L-dependent apoptotic pathway in DU145 cells (11). DU145 cells are resistant to apoptosis induced by anti-Fas-IgM but become sensitized to that IgM in the presence of camptothecin (9). Furthermore, DU145 cells may be induced to apoptose by tumor necrosis factor-related apoptosis-inducing ligand (12). The RC0.1 cell subline is a 9NC-SN38-topotecan-resistant derivative of the DU145 cell line selected after continuous incubation with 0.1 μM 9-nitro-camptothecin (9, 11). The top1 in RC0.1 (but not DU145) cells contains an R364H mutation that leaves the enzyme catalytically active but resistant to inhibition by camptothecin analogues in biochemical assays. The normal top1 allele is not expressed in RC0.1 cells (5). However, identification of the R364H mutation does not rule out the possibility that additional molecular changes also contribute to the observed camptothecin resistance.

In this study, we demonstrate a difference in the profiles of mRNAs expressed in DU145 and RC0.1 cells using 1648-clone cDNA microarrays designed to focus on cancer-interesting genes. One hundred eighty one genes differed in expression level by a factor of ≥1.5 between the two cell types. When the genes in the array were classified by function, we identified several categories that contained a higher percentage (*i.e.*, with $P < 0.05$) of the 181 changing genes than would have been expected by chance. The largest such class was that of the apoptotic genes ($P = 0.04$). Because camptothecin treatment

Received 8/26/02; accepted 1/2/03.

The costs of publication of this article were defrayed in part by the payment of page charges. This article must therefore be hereby marked *advertisement* in accordance with 18 U.S.C. Section 1734 solely to indicate this fact.

[1] To whom requests for reprints should be addressed, at Laboratory of Molecular Pharmacology, Center for Cancer Research, National Cancer Institute, NIH, Building 37, Room 5056, Bethesda, MD 20892-4255. Phone: (301) 496-9572; E-mail: wcr@mail.nih.gov (to W. C. R.) and Phone: (301) 496-9571; E-mail: jw4i@nih.gov (to J. N. W.).

[2] Present address: University of California San Francisco Cancer Center, San Francisco, CA 94122.

[3] Present address: Genome Institute of Singapore, Science Park II, 117528, Singapore.

[4] The abbreviations used are: top1, topoisomerase I; FACS, fluorescence-activated cell sorter; RT-PCR, reverse transcription-PCR; TUNEL, terminal deoxynucleotidyl transferase-mediated nick end labeling; BrdUrd, bromodeoxyuridine; APO, apoptosis; NFκB, nuclear factor κB; PI3K, phosphatidylinositol 3′-kinase; TGF, transforming growth factor; IκB, inhibitor of nuclear factor-κB; JNK, c-Jun NH_2-terminal kinase.

(4), in addition to many other chemotherapies and irradiation, has been shown to induce apoptosis (4), we asked if a generalized functional shift in apoptotic response had occurred between DU145 and RC0.1 cells.

MATERIALS AND METHODS

Reagents for Cell Treatments and Flow Cytometry Studies. Cell culture medium RPMI 1640 was from BioWhittaker, (Walkersville, MD); fetal bovine serum from Atlantic Biologicals (Norcross, GA); L-glutamine from Life Technologies, Inc. (Rockville, MD); trypsin-EDTA solution from Quality Biologicals, Inc. (Gaithersburg, MD); camptothecin, staurosporine, *cis*-platinum (II)-diammine dichloride, DMSO, propidium iodide and RNase from Sigma-Aldrich (St. Louis, MO); the APO-BrdUrd kit from BioSource International, Inc. (Camarillo, CA); and Annexin V-FLUOS staining kit from Roche (Indianapolis, IN). The DU145 cell line was obtained from the American Type Culture Collection (Rockville, MD). The RC0.1 cell subline was derived from DU145 cells continuously exposed to 25 nM 9NC for 1 month, 50 nM 9NC for 3 months, and 0.1 μM 9NC for 3 months (13). In the present study, cells were cultured in RPMI 1640 containing 0.29 mg/ml L-glutamine and 10% fetal bovine serum, and harvested using trypsin-EDTA at 85% confluence. For studies of drug sensitivity, camptothecin, staurosporine, and *cis*-platinum were solubilized in DMSO and added to the cells for 48 h of continuous exposure before harvest. UVC irradiation at 254 nm was done with a UV Stratalinker 1800 (Stratagene, La Jolla, CA), and the cells were harvested after 48 h. γ-Irradiation was done with a 6000-Ci Cs137 Mark I irradiator, model 68 (J. L. Shepherd & Associates, San Fernando, CA), and the cells were harvested after 48 h. For serum starvation, cell cultures were divided into RPMI 1640 with L-glutamine, washed twice with PBS (Life Technologies, Inc.) the next day, incubated for 2 days in the medium, washed twice with PBS, incubated for 3 days in medium, and then harvested.

FACS Analysis of Cell Cycle Distribution. Adherent cells were removed after trypsinization and washed in PBS after gentle centrifugation at 610 $\times$ *g* for 5 min. The cell pellets were fixed by resuspending them in 0.5 ml of 70% ethanol for 30 min, centrifuging at 925 $\times$ *g* for 8 min, and washing twice with ice-cold PBS to remove residual ethanol. For cell cycle analysis, the pellets were resuspended in 0.5 ml of PBS containing 50 μg/ml of propidium iodide and 100 mg/ml of RNase, then incubated at 37°C for 30 min and studied using a FACScan flow cytometer (Becton Dickinson, San Jose, CA).

Reagents for cDNA Microarray Analysis. The RNeasy kit was from Qiagen (Valencia, CA); diethyl pyrocarbonate-treated water from Research Genetics (Huntsville, AL); Cy3-dUTP, Cy5-dUTP, deoxynucleotide triphosphates, oligo(dT)$_{12-18}$ and oligo(dA)$_{40-60}$ from Amersham Pharmacia Biotech (Piscataway, NJ); and reverse transcriptase Superscript II and hCOT-1 from Life Technologies, Inc.

cDNA Microarray Analysis of Gene Transcription. Total RNA was isolated from cells using the RNeasy kit and diluted to a concentration of 5 μg/μl in diethyl pyrocarbonate-treated water. In cDNA labeling reactions, 90 μg of total RNA were used for Cy5 labeling, and 78 μg of total RNA were used for Cy3 labeling. Seventy-five μM Cy3-dUTP or Cy5-dUTP were used in each labeling. Pairs of Cy3- and Cy5-labeled cDNA samples (DU145 and RC0.1 for the experimental microarrays) were mixed and hybridized to a pin-spotted cDNA microarray (Oncochip) developed in the Microarray Facility, Advanced Technology Center, National Cancer Institute, NIH, and prepared by one of us (W. C. R.). This glass slide microarray contained 2208 cDNA spots corresponding to 1648 individual human cancer-interesting genes (array lot HS-OC-2p10–101899).[5] Included were 780 spots representing 364 individual genes in replicate. Hybridization data were acquired using a GenePix 4000 fluorescence scanner (Axon Instruments, Inc., Union City, CA). Images were analyzed using software developed by Yidong Chen in the Laboratory of Cancer Genetics, National Human Genome Research Institute.[6] Validation studies were done by real-time RT-PCR as described in supplemental material.[7]

Data Normalization. Microarray data were preprocessed using the PreProc computer program developed by Lawrence H. Smith (National Cancer Institute, NIH, Bethesda, MD).[7] Options used included Gaussian kernel fitting, no background subtraction, and whole-chip data normalization (14). Gene ratios for four experimental arrays (*i.e.*, two color-reversed pairs) were reciprocally averaged.

Data Analysis. Because we had four array measurements (arrays 72, 73, 74, and 75) for each gene with three categories of expression ratio levels, we performed a repeated measures analysis to test the hypothesis of no association between the four arrays and three response levels, adjusted for gene. Thus, we obtained 1648 independent two-way contingency tables such that each table had four rows, one for each of the four arrays and three columns corresponding to the expression ratio levels. Each entry n_{hij} ($h = 1,\ldots,1648$; $i = 1,\ldots,4$; $j = 1,\ldots,3$) in the table was given a value of 1 when gene h was classified in expression ratio level j for array i, and 0 otherwise. We then applied the extended Mantel-Haenszel mean score statistic

$$f_{i.} = \sum_{h=1}^{1648} \sum_{j=1}^{3} a_{hj} n_{hij}$$

for $i = 1,\ldots,4$; where $\{a_{hj}\}$ is the set of scores for response levels in the hth stratum. Because the distribution of genes was not uniform over the three levels of expression ratio, we used rank scores standardized by the sample size in a nonparametric analysis. Because the across-strata sample sizes

$$n_{i.} = \sum_{h=1}^{1648} \sum_{j=1}^{3} n_{hij}$$

$i = 1,\ldots,4$, were sufficiently large, the quantity

$$Q = \frac{(f_{i.} - \mu_*)^2}{v_*}$$

had approximately a χ^2 distribution with three degrees of freedom, where μ_* is the expected value of $f_{i.}$ with variance v_* under the null hypothesis of no association (see Ref. 15). An analogous formula was used to incorporate the adjustment of the reciprocal indicator variable with the corresponding number of degrees of freedom. This treatment assumes, as is often done, that the overall covariance of expression patterns among different genes is negligible in comparison with the total variance. All of the analyses were done using SAS software version 8.2.

Gene Functional Assessment. Genes were assessed functionally based on molecular pathway information developed by Kohn (16).[7] Additional assessments were made using GeneCards[8] and MedMiner (17).[7]

APO-BrdUrd (TUNEL) and Annexin V FACS Assays. Adherent cells were removed after trypsinization, collected in PBS, centrifuged at 610 $\times$ *g* for 5 min, fixed in 70% ethanol for 30 min, washed twice with cold PBS, resuspended in 0.5 ml of PBS with 50 μg/ml of propidium iodide and 100 mg/ml of RNase, incubated at 37°C for 30 min, and analyzed using a FACScan flow cytometer. The APO-BrdUrd assay was performed using the APO-BrdUrd kit following instructions of the manufacturer. In brief, DNA strand fragments in the cells were tagged with BrdUrd-dUTP at their 3′-OH ends using terminal deoxynucleotidyl transferase. The BrdUrd-dUTP was fluorescein-labeled with a monoclonal antibody to BrdUrd, and the cells were then analyzed in a FACScan flow cytometer. Phosphatidylserine translocation was measured using the Annexin V-FLUOS staining kit for fluorescence labeling and the FACScan for measurement of the resulting fluorescence.

RESULTS

Flow Cytometry Indicates Resistance of RC0.1 Cells to Camptothecin-induced Apoptosis. After 48 h of continuous exposure to 20 nM and 100 nM camptothecin, the parental DU145 cells showed dramatic arrest in late S phase and early S phase, respectively, and the emergence of presumably apoptotic cells with DNA contents lower than that of cells in G_1 phase (Fig. 1). After treatment with 100 nM camptothecin, there was a 74% reduction in DU145 cell number at

[5] Internet address: http://nciarray.nci.nih.gov/gi_acc_ug_title.shtml.
[6] Internet address: http://www.nhgri.nih.gov/DIR/LCG/15K/HTML/protocol.html.
[7] Internet address: http://discover.nci.nih.gov.
[8] Internet address: http://bioinformatics.weizmann.ac.il/cards.

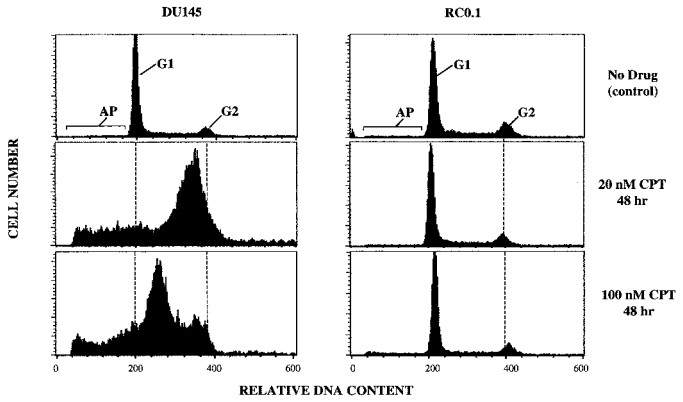

Fig. 1. Flow cytometric analysis of the cell cycle profiles of DU145 and RC0.1 cells treated with camptothecin. DU145 and RC0.1 were exposed to 20 or 100 nM camptothecin for 48 h, then harvested, stained with propidium iodide, and analyzed for perturbations in the cell cycle and for presence of apoptotic cells. From the histograms shown in this figure, we calculated that in untreated (control) cells the G_1, S, and G_2 fractions were 72, 16, and 10% for DU145, and 63, 14, and 15% for RC0.1. The apoptotic fractions (*AP*) at 0, 20, and 100 nM camptothecin were 0, 17, and 24% for DU145, and 3, 2, and 6% for RC0.1. Note that camptothecin, at both concentrations, resulted in accumulation of DU145 (but not RC0.1) cells in S phase.

48 h in comparison with untreated DU145. In contrast, the resistant subline, RC0.1, showed no discernible treatment-related change in cell cycle distribution and only a 17% reduction in cell number. The percentages of cells with sub-G_1 DNA contents after treatment with 20 nM and 100 nM camptothecin were 17% and 24% for DU145 and 2% and 6% for RC0.1. As with many pharmacological experiments, a reduction in cell number (as seen here for DU145 cells) may have reflected a selection process for cells less affected by the drug. That selection process would be expected to decrease the differences observed between wild-type and resistant variant.

Quadruplicate Microarray Analysis Identifies Gene Expression Differences of 1.5-fold or Greater between DU145 and RC0.1 for 181 Genes. To determine which genes might have been involved in the differential apoptotic response, we used cDNA microarrays to compare gene expression in RC0.1 and DU145. Two arrays were hybridized with Cy5-labeled DU145 cDNA and Cy3-labeled RC0.1 cDNA. Two arrays were labeled in the reciprocal way with Cy3-labeled DU145 cDNA and Cy5-labeled RC0.1 cDNA. For a "split sample" control, RC0.1 RNA was the source for both Cy5- and Cy3-labeled cDNA. Overall, we observed that 181 of 1648 (11.0%) of the genes differed in expression level by a factor of $\geq$1.5 between DU145 and RC0.1. Table 1*A* lists genes expressed at least 4-fold lower in RC0.1, and Table 1*B* lists genes expressed at least 4-fold higher in RC0.1. Also included are genes belonging to functional groups enriched or depleted to a statistically significant extent by $>$1.5-fold (see Table 3).

Three hundred sixty four genes were replicated at least once on the array. Of those, 312 showed agreement across all of the replicates with regard to classification as unchanged or altered by 1.5-fold (either up or down). Genes that showed disagreement were excluded from consideration unless they had also been evaluated by real-time RT-PCR. The median SD across replicates for the "mean intensity ratios" (see Table 1, *A* and *B*) was 0.12 (*i.e.*, 12%), indicating a high degree of reproducibility.

Replicate genes on the array that showed disagreement were deemed unreliable and excluded from the analysis, unless the disagreement was resolved by TaqMan real-time RT-PCR (data not shown). These RC0.1:DU145 ratios ranged from 0.13 to 13.1 and were consistent from one experimental array to the next. The median coefficient of variation for these 181 genes was 0.14 (*i.e.*, 14%). For the split sample, 2.9% of the genes exceeded the 1.5-fold change cutoff. Use of the reciprocal-labeling experimental design and analysis eliminated red-green bias for any particular spot. Some genes appeared multiple times on the array, thus providing $\geq$8-fold replication of the results.

The Overall Correlation of Microarray and Real-Time RT-PCR Data Is 0.89. To test the reliability of the microarray data, we used TaqMan real-time RT-PCR assay because it is highly specific, and because its sources of error are very different from those of hybridization to a cDNA array. There was a general concordance between microarray and real-time RT PCR results ($r = 0.89$ for the 18 genes studied; see data in Supplementary Table 2).[7] The overall Pearson correlation coefficient for the 18 gene ratios studied was 0.89 (data not shown). GSTP1, IL8, and NK4 differed most dramatically in expression between DU145 and RC0.1. The magnitude of the change was underrepresented by the microarrays, but the direction was correct. By real time RT-PCR, the RC0.1:DU145 ratios were 0.001, 0.002, and 0.03, respectively.

Analysis of Quadruplicate Arrays Yields a Reliable Assessment of Gene Expression Level Changes. The gene expression ratios in DU145 and RC0.1 cells were compared across the four microarrays, 72, 73, 74, and 75. Microarrays 72 and 73 had ratios of expression intensity (reciprocal indicator = R/G) based on fluorescent dyes that were reversed with respect to those of the other two microarrays, 74 and 75 (reciprocal indicator = G/R). These ratios were compared for the 1648 individual genes present on the microarray.

The ratios of expression intensity were divided into three categories ($'< 0.67'$, $'[0.67, 1.5]'$, $'> 1.5'$). Table 2 shows the overall distribution of expression ratios. Nonparametric analysis was used to test the null hypothesis of no association. We applied the stratum-adjusted Kruskal-Wallis (extended Mantel-Haenszel) test, considering each gene to constitute a stratum. Because the three ordered levels for the expression ratio are not equally spaced, rank scores standardized by sample size were used for the mean score statistics.

After combining values from microarrays 72 and 73, and values from microarrays 74 and 75, we observed an association between the ratio levels and the reciprocal indicator ($P = 0.0027$), indicating a small but statistically significant "dye-effect." After adjusting for the reciprocal indicator as well as the individual genes, we saw no association between the expression ratios and microarray number using the same nonparametric analysis ($P = 0.73$). We also saw no association between expression ratio and the microarray number within the two levels of the reciprocal indicator; that is, expression ratios had no association with microarray for arrays 72 and 73 ($P = 0.26$) or 74 and 75 ($P = 0.58$). This observation indicates that there was no significant array effect on the expression ratios.

There was a strong overall concordance in expression ratio level ($\kappa = 0.67$, where a value of 1 corresponds to perfect concordance and a value of 0 corresponds to that expected by chance, with 95% confidence interval, 0.64–0.71) between the gene ratios for microarrays 72 and 73, and between microarrays 74 and 75. Thus, the expression ratios of the four microarrays (after adjustment for the reciprocal indicator) were highly likely to fall into the same category (*i.e.*, one of the three levels). Both the association and concordance findings indicate reproducibility of the ratios for the individual genes across the four microarrays.

Five of 179 Functional Gene Categories Show Greater Than Expected Numbers of Expression Level Differences between DU145 and RC0.1 Cells. Functional classification of the genes present on the microarray (16) yielded 179 functional categories. We asked which of the categories were statistically significantly enriched for genes that had a $\geq$1.5-fold level of change with respect to the null hypothesis that the expected 11% of genes (181 of 1648) in the cat-

Table 1 *Microarray-determined levels of expression of genes differing by ≥1.5-fold between DU145 and RC0.1*

A. 25/79 genes expressed ≥1.5-fold lower in RC0.1 than in DU145: included are three genes spotted in duplicate[a]

	RC0.1:DU145 gene expression ratio									
Array 76 split sample	Array 72	Array 73	Array 74	Array 75	Mean 72–75	SE[b] 72–75	Coeff. Var[c] 72–75	Gene name	Clone ID	Module[d]
1.01	0.14	0.10	0.17	0.10	0.12[f]	0.02	0.25	Glutathione-*S*-transferase π-1[e]	774710	Ox
1.04	0.14	0.11	0.12	0.13	0.13[f]	0.01	0.10	NK4 = Natural killer cells protein-4	810859	na
1.04	0.13	0.11	0.15	0.12	0.13[f]	0.01	0.14	IL-8	328692	IL-8
1.15	0.22	0.20	0.17	0.23	0.20	0.01	0.14	T-cell receptor β chain[e]	302157	TCR
0.88	0.19	0.18	0.35	0.28	0.23	0.04	0.32	CARP = cytokine inducible nuclear protein	840683	na
1.17	0.29	0.31	0.16	0.29	0.24	0.04	0.27	Cyclin-dependent kinase 5 regulatory subunit	757873	Cdk
1.10	0.23	0.24	0.26	0.26	0.25	0.01	0.06	Fra-1	110503	FRA
1.03	0.24	0.26	0.27	0.31	0.27	0.01	0.11	Fra-1	110503	FRA
1.12	0.39	0.37	0.36	0.34	0.36[f]	0.01	0.06	IκB α	340734	NFKB
0.92	0.47	0.47	0.45	0.43	0.45[f]	0.01	0.05	BAD = bbc6 = proapoptotic Bcl-2 homolog	1286754	Appt-Mc
0.98	0.54	0.43	0.57	0.45	0.49	0.03	0.13	NFκB2 = NF-κB p100 = p49	682529	NFKB
0.97	0.49	0.46	0.56	0.48	0.50[f]	0.02	0.09	BAD = bbc6 = proapoptotic Bcl-2 homolog	301984	Appt-Mc
0.97	0.55	0.49	0.53	0.65	0.55	0.03	0.12	A20	141806	Appt-TNF
1.00	0.75	0.62	0.39	0.57	0.55	0.07	0.25	MHC class I = HLA-B27[e]	769753	MHC
1.09	0.60	0.47	0.67	0.56	0.57	0.04	0.14	MHC class II DR β5[e]	491166	MHC
0.90	0.65	0.49	0.62	0.59	0.58[f]	0.03	0.12	CASPASE-6 = mch2 α	323500	Appt-casp
1.16	0.54	0.55	0.62	0.63	0.58	0.02	0.07	cIAP1 = API1 = MIHB = IAP homologue B	34852	Appt-IAP
0.97	0.59	0.60	0.49	0.69	0.58	0.04	0.14	MHC class I protein HLA-G	1117041	MHC
1.01	0.67	0.60	0.59	0.54	0.60	0.03	0.09	relB = I-Rel[e]	66969	NFKB
1.01	0.62	0.56	0.59	0.68	0.61	0.03	0.08	IκB ϵ	993539	NFKB
1.26	0.62	0.81	0.46	0.63	0.61	0.07	0.23	Decoy receptor 2	1175007	Appt-TNF
0.97	0.67	0.63	0.58	0.62	0.62	0.02	0.05	MHC class I protein HLA-G	1117041	MHC
0.89	0.66	0.52	0.68	0.70	0.63	0.04	0.13	MHC class I = HLA-A2[e]	588819	MHC
0.86	0.55	0.60	0.74	0.72	0.64	0.05	0.15	MHC class II = DQ α[e]	756092	MHC
1.00	0.81	0.67	0.54	0.64	0.65	0.06	0.17	MHC class I = HLA-C4	810142	MHC
0.98	0.53	0.54	0.83	0.82	0.65	0.08	0.25	NFκB-p65 = RelA	771220	NFKB
1.02	0.67	0.65	0.71	0.64	0.66	0.02	0.05	MHC class II = DR α[e]	726209	MHC
0.98	0.68	0.61	0.65	0.72	0.67	0.02	0.07	Reqiem (HREQ)	25695	Appt

B. 20/102 genes expressed >1.5-fold higher in RC0.1 than in DU145: included are 6 spotted in duplicate[a]

	RC0.1:DU145 gene expression ratio									
Array 76 split sample	Array 72	Array 73	Array 74	Array 75	Mean 72–75	SE[b] 72–75	Coeff. Var[c] 72–75	Gene name	Clone ID	Module[d]
1.01	13.78	10.91	14.07	14.40	13.12	0.80	0.12	Human small GTP-binding protein rab30	U57092	Ras
1.08	13.83	10.97	12.35	13.99	12.66	0.71	0.11	Mitochondrial 1 25-dihydroxyvitamin D3 24-hydroxylase	266146	Mitochon
1.06	13.86	14.41	10.88	11.70	12.54	0.85	0.14	Mitochondrial 1 25-dihydroxyvitamin D3 24-hydroxylase	266146	Mitochon
1.06	6.13	7.10	11.64	14.45	8.71[f]	1.95	0.45	Glutathione peroxidase 2 gastrointestinal	587847	Ox
1.09	8.14	7.94	5.37	7.02	6.93	0.63	0.18	Histone 2A-like protein (H2A/I)	429091	Chtn
1.00	6.18	6.88	6.43	8.26	6.85	0.46	0.14	Histone 2A-like protein (H2A/I)	429091	Chtn
1.06	4.92	6.52	6.09	4.87	5.51	0.42	0.15	CHD2	293017	na
1.09	5.27	4.83	4.81	6.17	5.22[f]	0.32	0.12	EGR-1 = Early growth response protein 1 = zinc finger protein	376370	Early resp
1.05	5.35	4.96	5.23	5.31	5.21	0.09	0.03	(KIAA0324)—sequence verification failed	489453	na
1.12	6.13	4.69	4.41	5.47	5.09	0.39	0.15	(KIAA0324)—sequence verification failed	489453	na
0.98	3.33	4.15	4.12	5.73	4.17	0.50	0.24	GLUT3 = glucose transporter protein-3	259029	na
1.08	4.15	4.43	3.72	4.15	4.10	0.15	0.07	Cyclin D3	327182	Cdk-cyc
1.01	2.51	2.34	1.96	2.45	2.29[f]	0.12	0.11	Defender against cell death 1 = DAD 1[e]	209156	Appt-Dad
0.99	1.80	1.75	2.63	2.65	2.12	0.25	0.24	Defender against cell death 1 = DAD 1	341699	Appt-Dad
0.78	2.50	2.79	1.51	1.80	2.02	0.30	0.30	GTP:AMP phosphotransferase mitochondrial	295176	Mitochon
1.19	1.95	2.29	1.93	1.91	2.01	0.09	0.09	Mitochondrial serine hydroxymethyltransferase gene	267753	Mitochon
0.76	2.27	3.25	1.63	1.58	2.00	0.39	0.39	Decoy receptor 1 = DcR1 = TRAIL receptor 3[e]	470799	Appt-TNF
0.97	2.22	2.15	1.72	1.97	1.99	0.11	0.11	BCL-3	1133162	NFKB
1.10	2.08	1.64	1.97	1.67	1.82	0.11	0.12	Serine hydroxymethyl transferase mitochondrial precursor	344080	Mitochon
0.99	1.90	1.73	1.74	1.90	1.81	0.05	0.05	Serine hydroxymethyl transferase mitochondrial precursor	344080	Mitochon
0.92	1.73	1.92	1.68	1.65	1.74	0.06	0.07	Fra-2	271441	FRA
1.01	1.37	1.28	2.19	2.17	1.65	0.25	0.30	Bag-1 = Bcl-2 interacting protein = RAP46	469256	Appt-Mc
1.07	1.65	1.64	1.58	1.68	1.64	0.02	0.03	DAP-1	488754	Appt-TNF
0.98	1.89	1.97	1.25	1.41	1.57	0.18	0.23	BAG1 = Similar to mouse bcl-2 binding protein BAG-1	1322301	Appt-Mc
1.01	1.86	1.89	1.22	1.46	1.56	0.16	0.21	CD27BP (Siva)	501643	Appt
1.11	1.18	1.36	2.00	1.72	1.50	0.18	0.24	NIP2 = E1B 19K/Bcl-2-interacting protein	712232	Appt-Mc

[a] Only genes with >4-fold change, or from categories with statistically significant levels of change of ≥1.5-fold (see Table 4) included.
[b] SE is the standard error of the mean.
[c] Coefficient of variation.
[d] Modules defined in Table 4 functional analysis. Genes not assigned to a category are designated na.
[e] Sequence verification failed.
[f] Indicates a gene of which the direction of expression change has been verified by real time RT-PCR.

egory would differ in expression. Five of the 179 categories (Table 3) met that criterion: "apoptotic," "fra-2-associated," "MHC," "mitochondrial," and "NFκB-associated." For the statistical analysis, we used the one-tailed exact binomial test without correction for multiple comparisons. The one-tailed test was used because only categories with proportions statistically >11.0% (181 of 1648) were a point of focus in our attempt to explain the observed shift in apoptotic response.

RC0.1 Cells Are Markedly Resistant to Induction of Apoptosis by Various Cytotoxic Agents and Metabolic Stresses. To test whether the statistical indications of alteration in the apoptotic pathway had functional implications, we assessed the apoptotic responses

Table 2 *Distribution of microarray gene expression ratios*

	<0.67[a]	[0.67, 1.5][a]	>1.5[a]	Total
Microarrays 72, 73, 74, and 75 total gene expression ratio distribution				
72[b]	105 [6.4]	1421 [86.2]	122 [7.4]	1648
73[b]	111 [6.7]	1396 [84.7]	141 [8.6]	1648
74[c]	135 [8.2]	1377 [83.6]	136 [8.3]	1648
75[c]	132 [8.0]	1390 [84.3]	126 [7.7]	1648
Microarrays 72 *versus* 73 gene expression ratio distribution[d]				
<0.67	76 [72.4]	29 [27.6]	0 [0.0]	105
[0.67, 1.5]	35 [2.5]	1342 [94.4]	44 [3.1]	1421
>1.5	0 [0.0]	25 [20.5]	97 [79.5]	122
Microarrays 74 *versus* 75 gene expression ratio distribution[e]				
<0.67	90 [66.7]	45 [33.3]	0 [0.0]	135
[0.67, 1.5]	42 [3.1]	1303 [94.6]	32 [2.3]	1377
>1.5	0 [0.0]	42 [30.9]	94 [69.1]	136

[a] Values represent number of genes present on the microarray that fall within the defined expression ratio category, followed by the percentage of the total number of genes in parentheses. All ratios are presented as RC0.1/DU145.
[b] Hybridized with cy5-labeled DU145 cDNA and cy3-labeled RC0.1 cDNA.
[c] Hybridized with cy3-labeled DU145 cDNA and cy5-labeled RC0.1 cDNA.
[d] Rows are microarray 72, columns are microarray 73.
[e] Rows are microarray 74, columns are microarray 75.

to various treatments by flow cytometry using the Annexin V fluorescence assay to detect early apoptosis events (*i.e.*, phosphatidylserine translocation to the outer plasma membrane leaflet) and the APO-BrdUrd (TUNEL) assay for detection of late apoptosis events (*i.e.*, chromosomal DNA fragmentation). Fig. 2*A* indicates early apoptosis events in DU145 cells subjected to diverse treatments, including exposure to camptothecin, staurosporine, and cisplatin, as well as serum starvation, and UV and γ-irradiation. The most extensive response was observed in staurosporine-treated DU145 cells. In contrast, practically no late apoptosis was seen in RC0.1 cells exposed to camptothecin, cisplatin, serum starvation, or γ-irradiation (see histograms in Fig. 2*A*). Staurosporine and UV irradiation induced the signature of late apoptosis in RC0.1 cells (Fig. 2*A*). The results are summarized quantitatively in Table 4.

The PI3K Inhibitor Wortmannin Potentiates the Apoptotic Response to Camptothecin. The PI3K molecule falls within the area of the molecular interaction map that changes in a direction consistent with the observed shift in apoptotic response. The apoptotic response to camptothecin treatment in the presence of wortmannin, an inhibitor of PI3K (18), was assessed by flow cytometry using the Annexin V and APO-BrdUrd assays. Wortmannin dramatically increased the apoptotic response of DU145 cells, particularly the late stage of apoptosis (Fig. 3, *A* and *B*). In contrast, wortmannin had no effect on apoptosis in RC0.1, with or without camptothecin. The apparent potentiation in DU145 cells suggests (but does not prove) PI3K involvement in the resistance of RC0.1 cells to camptothecin. In other experiments (see supplemental material[7], Figs. 2A and B), wortmannin similarly potentiated *cis*-platinum-induced apoptosis in DU145 but not RC0.1, suggesting a defect in RC0.1 that relates directly to, or is downstream from, PI3K.

DISCUSSION

Differences between DU145 and RC0.1 Cells in Gene Expression and Susceptibility to Apoptosis. This study started with a comparison of gene expression profiles in the DU145 human prostate cancer cell line and a subline, RC0.1, selected for resistance to camptothecin (5). RC0.1 cells express top1 with a mutation that does not alter the catalytic activity of the enzyme but confers resistance to camptothecin analogues in biochemical assays (5). However, that mutation does not exclude the possibility that additional molecular changes also contribute to the observed resistance. To identify such changes, we assessed gene expression profiles in the cells using quadruplicate Oncochip cDNA microarrays. Expression level differences by a factor of ≥1.5 between the two cell lines were prominent for several categories of functional genes (Table 3): apoptosis-related (12 of 62 genes; $P = 0.038$), MHC (7 of 15 genes; $P = 0.001$), mitochondria-related (but not apoptosis-related; 4 of 7 genes; $P = 0.004$), NFκB-related (6 of 14 genes; $P = 0.002$), and fra-2 associated (2 of 2 genes; $P = 0.012$). The apoptosis-related group was particularly interesting because of its relevance to drug resistance and because it was the largest group of genes that showed statistically significant enrichment with genes that differed in expression by a factor ≥1.5 between the two cell lines. Given the unique status of the apoptosis category, no correction for multiple comparisons was applied. However, in interpreting these *P*s, it is worth noting that the assumption of independence probably fails (to some unknown degree) for this calculation. Hence, the *P*s should be considered as heuristic indices, not as the results of formal inference.

Because changes in expression were prominent for genes associated with apoptosis, we next compared the apoptotic responsiveness of DU145 and RC0.1 cells after exposure to various drugs or other stressors (Fig. 2, *A* and *B*). Apoptotic response was markedly reduced in RC0.1, not only in response to camptothecin (top1 poisoning), but also in response to cisplatin (DNA cross-linking), staurosporine (protein kinase inhibition), serum starvation (growth factor deprivation), UV radiation (DNA cross-linking and major strand breakage), and ionizing radiation (DNA strand breakage). This pervasive functional response would not have been expected on the basis of the known top1 mutation.

Molecular Interaction Map of Apoptosis-related Gene Expression Patterns. The relatively large number of apoptosis-related genes that differed in expression between DU145 and RC0.1 cells was puzzling for two reasons. First, it was not clear why expression changes in so many genes would be required to achieve resistance to apoptosis. Second, many of the expression differences seemed to be in the direction contrary to what would be expected given the resistance of RC0.1 cells to apoptosis. To address these findings systematically, we constructed a molecular interaction map of the relevant apoptosis-

Table 3 *Functional[a] classification of genes*

Category[b] Name		Genes in category	Genes that differed by ≥1.5-fold	Genes expected to differ by ≥1.5-fold[c]	Exact binomial test *P*[d]
Apoptotic	Appt	62	12	6.8	0.038
fra-2 associated	FRA	2	2	0.2	0.012
Major histocompatibility complex	MHC	15	7	1.7	0.001
Mitochondrial	Mitochon	7	4	0.8	0.004
NFKB associated	NFκB	14	6	1.5	0.002

[a] Classification of genes done on a combined functional/structural analysis.
[b] Categories with a $P > 0.05$ are not shown.
[c] Expected number of genes based on the 11% (181/1648) of all genes found to have changed (Table 1, *A* and *B*).
[d] Based on the exact binomial test (implemented in S-Plus). The null hypothesis is that the observed proportion is ≤11% of genes in the category differed by ≥1.5-fold.

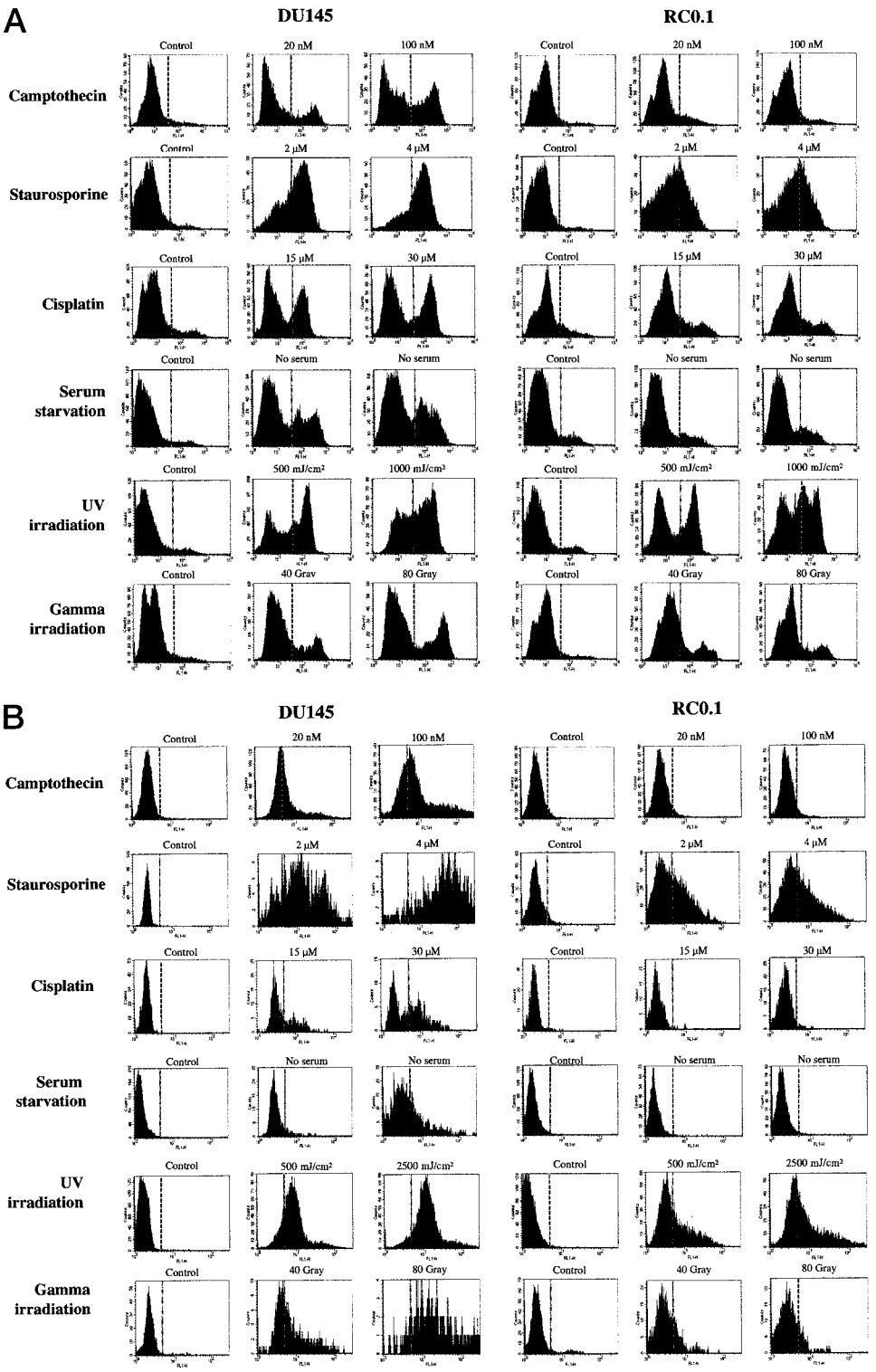

Fig. 2. Flow cytometric assays for apoptosis in DU145 and RC0.1 cells. The cells were treated with camptothecin, staurosporine, cisplatin, UV irradiation, γ-irradiation, or serum starvation as described in "Materials and Methods." Number of cells is indicated on the *Y*-axis. *A*, Annexin-V assay (early apoptosis). The logarithm of fluorescence intensity in the FL1-H channel (*X*-axis) is an indicator of phosphatidylserine translocation (early apoptosis event). *B*, Apo-BrdUrd (TUNEL) assay for DNA strand breaks (late apoptosis). The *X*- and *Y*-axes are as in *A* except that fluorescence intensity reflects DNA fragmentation. ···· mark the approximate upper limits of intensity for the no-stimulus (*control*) cell peaks.

related pathways, based on evidence cited in recent literature (Fig. 4*A*). The map, which can be found in a navigable electronic form,[7] was prepared using the notation of Kohn (16). Definitions of the symbols used are summarized in Fig. 4*B*. The molecular species associated with significant gene expression differences can be located via the map coordinates listed in Fig. 4*C*. In the map, the observed RC0.1:DU145 (R/D) gene expression ratios are in brackets within the molecular species symbols. The major findings, summarized in Fig. 4*C*, reflect the complexity of the biological system. It will be necessary to discuss those complexities here in some detail.

The Caspase and Bcl-2 Families. For these gene families, which affect apoptosis most directly, our microarray data included the following (R/D = ratio of mRNA levels in RC0.1:DU145). Proapoptotic genes: A1/Bfl-1 (R/D = 0.76), Bad (R/D = 0.50, 0.45), Bak (R/D = 0.86), Bik (R/D = 1.09), caspase-1 (R/D = 1.09), caspase-3 (R/D = 0.74), caspase-4 (R/D = 0.89), caspase-5 (R/D = 0.95), caspase-6 (R/D = 0.58), caspase-7 (R/D = 0.95), caspase-8 (R/D = 0.90), caspase-9 (R/D = 0.90), and caspase-10 (R/D = 0.84, 0.88). Antiapoptotic gene: Bcl-2 (R/D = 1.48, 1.32). Pro- and antiapoptotic isoforms: Bcl-x (R/D = 1.10).

Table 4 *Differences between RC01 and DU145 from Annexin-V and APO-BRDU assay profiles in Fig. 2*

The ratio of apoptotic response between DU145 and RC0.1 = $(\mathbf{A}_{\text{RC0.1-treated}}/\mathbf{A}_{\text{RC0.1-control}})/(\mathbf{A}_{\text{DU145-treated}}/\mathbf{A}_{\text{DU145-control}})$, where **A** is the percentage of cells to the right of the dotted line in Fig. 2, *A* and *B*.

	Ratio of apoptotic responses (RC0.1:DU145)			
	Annexin-V assay		TUNEL assay	
Apoptotic triggers	Condition 1	Condition 2	Condition 1	Condition 2
Camptothecin[a]	0.46	0.20	0.18	0.04
Staurosporine[a]	0.42	0.42	0.02	0.02
Serum Starvation[b]	0.23	0.29	0.18	0.06
Cisplatin[a]	0.53	0.48	0.02	0.04
UV Irradiation[c]	0.63	0.63	0.16	0.20
γ irradiation[c]	0.72	0.39	0.17	0.01

[a] Conditions 1 and 2 are the two drug concentrations (Fig. 2, *A* and *B*).
[b] Conditions 1 and 2 are duplicate assays (Fig. 2, *A* and *B*).
[c] Conditions 1 and 2 are the two irradiation levels (Fig. 2, *A* and *B*).

We see that 2 of these 14 genes exhibited ≥1.5-fold expression differences: BAD and caspase-6 (in the right lower quadrant of Fig. 4*A*). Both are proapoptotic genes that show reduced expression (R/D <0.67) in the apoptosis-resistant RC0.1 cells. These differences are therefore in the expected direction. The reduced expression of BAD in RC0.1 cells was confirmed by real-time RT-PCR, which gave a ratio R/D = 0.12 (see supplemental material).[7] The difference for antiapoptotic Bcl-2 was also in the expected direction (R/D = 1.32, 1.48), although the magnitude of the observed difference did not quite meet our threshold criterion of 1.5. However, the significance of this change is supported by the similar increase in mRNA level of c-Myb (R/D = 1.28, 1.48; Fig. 4*A*, *coordinates 8D*), a transcriptional activator of Bcl-2.

Gene Expression Differences Affecting the Proapoptotic Bcl-2 Family Member BAD. BAD is induced by staurosporine to migrate to mitochondria in prostate cells (19, 20), and it is up-regulated by serum starvation, leading to apoptosis (21). Several genes exhibited coherent expression differences stemming from reduced BAD mRNA levels in RC0.1 cells. (By "coherent" we refer to multiple pathways leading to the same effect; thus, multiple expression differences that have a common final molecular impact would be considered coherent.) Two Bcl-2-binding proteins, Bag1 and 53BP2, exhibited significantly different mRNA levels in RC0.1 and DU145 cells. Bag1, which binds Bcl-2 and inhibits apoptosis (22), was expressed at a higher level in RC0.1 for two different clones on the array (R/D = 1.65, 1.57). In contrast, 53BP2, which binds Bcl-2 and enhances doxorubicin-induced apoptosis (23), was expressed at a lower level in RC0.1 cells (R/D = 0.58). Therefore, these differences were in the expected direction (Fig. 4*A*, *lower right quadrant*). Coherent with the reduced expression of BAD in RC0.1 cells, we observed expression differences in 3 genes that could suppress the proapoptotic effect of BAD by way of Akt/PKB, a kinase that inhibits BAD by phosphorylation of critical sites. These 3 genes are phosphoinositide-3-kinase (PI3K catalytic γ-polypeptide; R/D = 1.60), integrin-β1 (R/D = 2.78), and receptor tyrosine kinase RON (R/D = 2.53). These genes appear to suppress BAD function by the mechanism indicated in the upper right quadrant of Fig. 4*A*. PI3K phosphorylates phosphatidylinositols at the 3′ position, thereby generating binding and activation sites for Akt/PKB. Although the role of integrins in apoptosis is complex (*e.g.*, see Ref. 24), the increased expression of integrin-β1 and RON in RC0.1 cells is noteworthy because these two receptors can cooperate to inhibit BAD by way of the Akt/PKB pathway (25, 26). Therefore, the expression differences of these 3 genes were in the expected direction and could additionally reduce the proapoptotic activity of already lowered levels of BAD. Thus, the reduced susceptibility of RC0.1 cells to apoptosis may have been attributable in part to reduced activity of BAD.

Effect of Wortmannin. Because expression of PI3K was greater in RC0.1 than in DU145, we exposed the cells to wortmannin, a PI3K inhibitor, in the presence and absence of camptothecin. Wortmannin potentiated apoptosis in DU145 cells (as assessed by the TUNEL assay), as predicted. That is, wortmannin appeared to inhibit a survival signal that is transmitted by or through PI3K to Akt/PKB (Fig. 4*A*, *top right quadrant*). Similarly, wortmannin potentiated cisplatin-induced apoptosis (see Supplemental Material, Fig. 6, *A* and *B*),[7] indicating that the suggested PI3K involvement is not limited to top1-active agents.

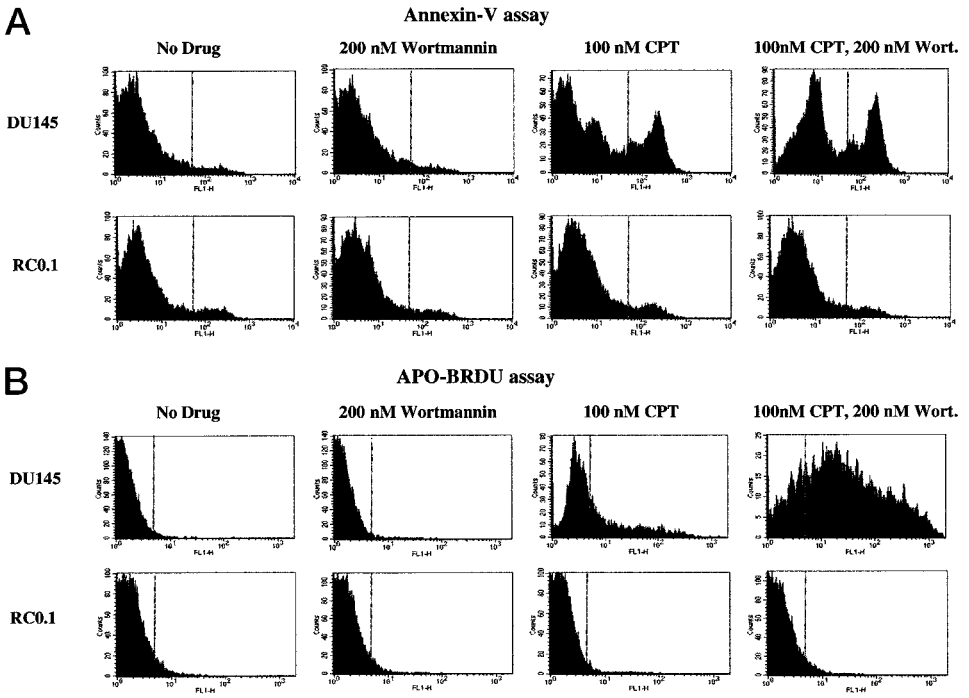

Fig. 3. The effect of treatment with wortmannin on camptothecin-induced apoptosis in DU145 and RC0.1 cells. Flow cytometric studies were done as described for Fig. 2. *A*, Annexin-V assay. *B*, APO-BrdUrd assay.

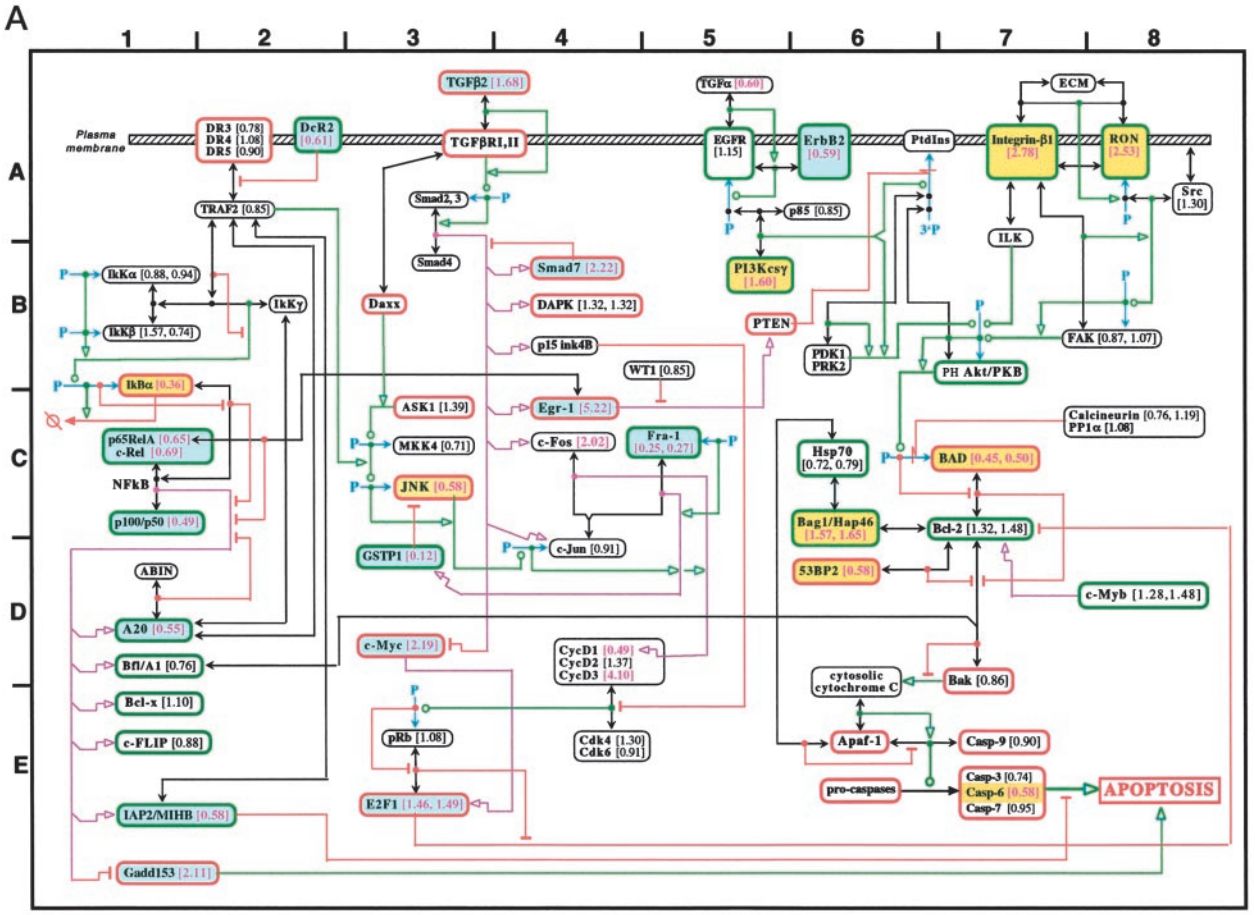

B

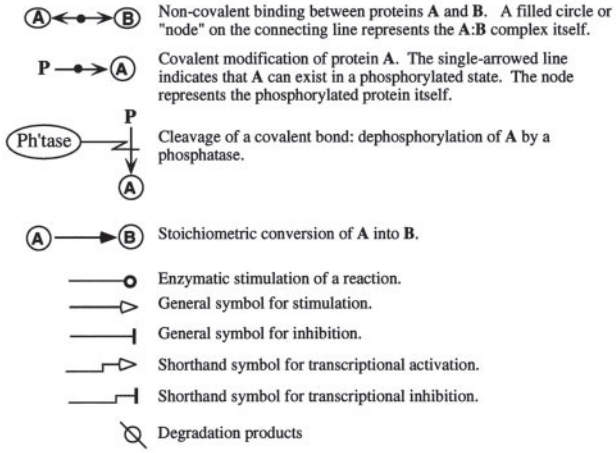

C

Gene[1]	Coordinates[2]	RC0.1/DU145[3]	Apoptosis[4]	Difference[5]
IkBα	1C	0.36	pro-	expected
p65RelA	1C	0.65	anti-	contrary
c-Rel	1C	0.69	anti-	contrary
p100/p50NFkB	1C	0.49	anti-	contrary
A20	1D	0.55	anti-	contrary
IAP2	1E	0.58	anti-	contrary
Gadd153	1E	2.11	pro-	contrary
DcR2	2A	0.61	anti-	contrary
TGFβ2	3A	1.68	anti-	contrary
JNK	3C	0.58	pro-	expected
GSTP1	3D	0.12	anti-	contrary
c-Myc	3D	2.19	pro-	contrary
E2F1	3E	1.48	pro-	contrary
Smad7	4B	2.22	pro-	contrary
Egr-1	4C	5.22	pro-	contrary
Fra-1	5C	0.26	anti-	contrary
PI3Kcs	5B	1.60	anti-	expected
ErbB2	6A	0.59	anti-	contrary
Bag1	6C	1.61	anti-	expected
53BP2	6D	0.58	pro-	expected
Integrin-β1	7A	2.78	anti-	expected
BAD	7C	0.48	pro-	expected
Caspase-6	7E	0.58	pro-	expected
RON	8A	2.53	anti-	expected

[1] Apoptosis-related genes exhibiting >=1.5 fold differences in mRNA levels between RC0.1 and DU145 cells.
[2] Coordinates of the gene on the molecular interaction map.
[3] Ratio of mRNA levels determined by microarray.
[4] Most prominently pro- or anti-apoptotic.
[5] "Expected" means that antiapoptotic gene was expressed more in RC0.1 than in DU145 cells, or proapoptotic gene was expressed less in RC0.1 than in DU145 cells.

Fig. 4. Molecular interaction map of the apoptosis-related pathways in which gene expression differences were observed. *A*, molecular interaction map. The observed gene expression ratios are shown in *brackets* next to the molecular species names, and the numbers are *highlighted in purple* when the expression differed by a factor of $> = 1.5$ in either direction. Molecules reported to favor or suppress apoptosis are bordered in *red* or *green*, respectively. When the mRNA expression change was in the expected direction, the gene symbol is *shaded yellow*; when in the contrary direction, it is *shaded blue*. *B*, summary of symbol definitions. For details, see Kohn (16). Although the symbol definitions are independent of color, we have adopted the following color convention to improve clarity. *Red*, inhibitory interaction; *green*, stimulatory interaction; *purple*, transcriptional stimulation; *black*, binding interaction. *C*, index of molecule coordinates on the map and summary of apoptosis relationships. The *top section* of the table contains molecules located on the *left* side of the map; most of these are NFκB-related, antiapoptotic, and contrary in their direction of change. The *middle section* of the table contains molecules located near the *horizontal center* of the map; many of these are TGFβ-related, and nearly all exhibited expression differences in the contrary direction. The *bottom section* contains molecules located on the *right* side of the map; most of these are in the apoptosis effector system (*bottom half* in the map) or signal through Akt/PKB (*top half* in the map), and nearly all exhibited expression differences in the expected direction.

Gene Expression Differences in the Contrary Direction. The gene expression differences considered thus far were consistent with the hypothesis that the apoptosis resistance of RC0.1 cells is largely because of reduced expression and/or enhanced post-transcriptional suppression of BAD. We now focus on the remaining apoptosis-related genes that exhibited differences. Unexpectedly, most of those genes exhibited differences in the contrary direction. Most are located on the left half of the map (Fig. 4*A*, *blue-shaded genes*). Many of them fall into two coherent groups governed by the NFκB and TGF-β transcription pathways.

Gene Expression Differences in the NFκB Pathway. In the NFκB pathway (Fig. 4*A*, *left side*), we see reduced expression in RC0.1 cells of three components of the NFκB transcription factors, namely p65RelA, c-Rel, and their transcriptional partner p100/p50. Although there was reduced expression of IκBα, a change that would tend to increase NFκB activity, the mRNA levels of NFκB transcription products were reduced (see below), suggesting that IκBα level may not have been limiting in this case.

The NFκB-stimulated transcription products for which we have data include A20, IAP2/MIHB, Bfl/A1, and c-FLIP. These genes have been reported as antiapoptotic. In addition, we have data for the NFκB-inhibited transcription product, Gadd153/CHOP, which has proapoptotic effects. A20, IAP2/MIHB, and Gadd153/CHOP showed expression differences $\geq$1.5-fold.

A20 and IAP2/MIHB inhibit apoptosis, and their transcription is positively controlled by NFκB (27, 28). A20 is a cytoplasmic zinc finger protein that inhibits tumor necrosis factor-stimulated apoptosis (29). IAP2/MIHB is a general caspase inhibitor. Gadd153/CHOP enhances apoptosis, and its transcription is negatively controlled by NFκB (30, 31). Gadd153/CHOP down-regulates Bcl-2 and sensitizes cells to apoptosis induced by stress at the level of the endoplasmic reticulum (31).

All of these differences are in a direction consistent with reduced NFκB transcriptional activity in RC0.1 cells. It is noteworthy that the mRNA level of *IAP2/MIHB*, a gene stimulated by NFκB, was diminished, whereas the mRNA level of *Gadd153/CHOP*, a gene inhibited by NFκB, was elevated. The decreased activity of the NFκB pathway in RC0.1 cells was unexpected because NFκB activity has mainly antiapoptotic effects (see Ref. 32). Another factor that may have contributed to down-regulation of NFκB-dependent transcription was the observed increase in the mRNA level of Egr-1 (R/D = 5.22). Egr-1 has been reported to bind p65RelA and thereby inhibit NFκB function (33). Egr-1 will be additionally considered in the context of the TGF-β pathway. In summary of this section, the NFκB pathway operates in the contrary direction with respect to the apoptosis resistance of RC0.1 cells.

Gene Expression Differences in the TGFβ Smad and AP-1 Pathways. The TGFβ-Smad pathway is noted for its proapoptotic effects in epithelial cells (34). In this pathway, we found increased expression of TGFβ2, Egr-1, Smad7, and c-Fos. The latter 3 genes are controlled by the Smad2/3:Smad4 transcription factors in response to TGFβ (Fig. 4*A*).

Egr-1 has a radiation-inducible promoter, and it enhances apoptosis in response to ionizing radiation in human PC-3 prostate cancer cells (35). Egr-1 may enhance apoptosis via at least two routes shown in Fig. 4*A*: (*a*) it stimulates transcription of PTEN, an indirect inhibitor of Akt/PKB (36); and (*b*) it binds and inhibits the RelA subclass of NFκB (33). Thus, the difference in Egr-1 expression (R/D = 5.22, one of the largest differences in our data set) was in the contrary direction.

Smad7, a feedback inhibitor of the TGFβ pathway, was up-regulated in RC0.1 (37), suggesting that increased transcription in these cells dominates over the feedback inhibition. Smad7 has proapoptotic actions via unknown connections to the JNK pathway (38) or possibly by reducing the antiapoptotic effect of the NFκB pathway (39). Either way, the increased Smad7 mRNA level in RC0.1 cells was in the contrary direction.

The relationship of c-Fos to apoptosis is complex. c-Fos binds c-Jun to form the AP-1 transcription factor, and the activity of c-Jun requires that it be phosphorylated by JNK (40). AP-1 can have pro- or antiapoptotic effects under different circumstances (41, 42). JNK generally has proapoptotic effects, some of which may be mediated via AP-1 (41, 43). c-Fos mRNA is controlled transcriptionally and also by mRNA stabilization in response to DNA damage (44). Thus, the increased level of c-Fos mRNA in RC0.1 cells cannot simply be assigned to a pro- or antiapoptotic category.

A Smad-independent pathway from TGFβ to apoptosis may go by way of Daxx and JNK, perhaps through a phosphorylation sequence involving ASK1 and MKK4 (Fig. 4*A;* Ref. 45). Daxx, which binds to the cytoplasmic domain of TGFβRII, can mediate TGF-β-induced apoptosis by stimulating JNK via ASK1 (see Ref. 46 and references cited therein). JNK is mainly proapoptotic (42). It activates c-Jun by phosphorylation of Ser-63 and Ser-73, and may thereby exert some of its proapoptotic effects (41, 42). The activity of the c-Fos:c-Jun heterodimer at AP-1 promoter elements may have been additionally increased in the RC0.1 cells by the reduced expression of Fra-1, a close relative of c-Fos. Like c-Fos, Fra-1 forms heterodimers with c-Jun, and it binds the same AP-1 promoter sites. Fra-1 has a transactivation domain that requires phosphorylation for activity. It may competitively inhibit AP-1 promoters (47). However, when its transactivation domain is phosphorylated, it may activate some promoters, such as that of GSTP1 (discussed below).

E2F-1 and c-Myc are prominent stimulators of apoptosis. Both had mRNA levels higher in RC0.1 than in DU145 cells, the contrary direction. c-Myc is a transcription factor that may contribute to up-regulation of E2F1 (Ref. 48; Fig. 4*A*). The c-*myc* promoter contains an inhibitory Smad-binding element and, thus, may be down-regulated by TGF-β (49). However, despite the elevated activity in the TGF-β-Smad pathway, c-*myc* mRNA levels were elevated in RC0.1 cells. This increase may have been because of post-transcriptional regulation, because c-*myc* mRNA and protein both are short-lived, and regulation by mRNA stabilization has been reported (44).

The increased E2F1 mRNA level in RC0.1 cells was consistent with the increased c-*myc* mRNA level, because c-*Myc* has been reported to increase E2F1 mRNA levels (48). Moreover, Myc-induced apoptosis requires E2F1 (48). c-Myc and E2F1 may have stimulated apoptosis by suppression of Bcl-2 mRNA and protein (50, 51).

The contrary elevation of E2F1 and c-*myc* mRNAs in RC0.1 are the most striking of the seemingly paradoxical changes that we observed. However, we consider next an almost equally unexpected contrary reduction of GSTP1.

Gene Expression Differences in GSTP1. The glutathione *S*-transferase gene, *GSTP1,* was markedly suppressed in RC0.1 cells (R/D = 0.12 by microarray; ~0.001 by real-time RT-PCR). *GSTP1* protects cells against apoptosis induced by oxidative stress or DNA-damaging drugs (52). Therefore, the markedly reduced *GSTP1* mRNA level in RC0.1 cells is in the contrary direction. Protection against apoptosis by *GSTP1* may be attributable, in part, to inhibition of JNK. Inhibition of JNK by *GSTP1* is abrogated by oxidative stress, which causes *GSTP1* to form covalent dimers that cannot interact with JNK (53, 54). An AP-1 site in the *GSTP1* promoter can be activated by Fra-1:c-Jun heterodimer (55). Thus, the reduced *GSTP1* mRNA level may have been attributable in part to lower Fra-1 mRNA. Fra-1 has a transactivation domain that can be activated through phosphorylation by ERK (56). *GSTP1,* which is expressed in DU145 cells, can be silenced by hypermethylation of CpG islands, particularly in prostate cancer (57–59). We are investigating whether the contrary decrease in

GSTP1 mRNA in RC0.1 cells was because of hypermethylation, an epigenetic event that has a relatively high probability of spontaneous occurrence.

The Apoptosis-related Gene, *Dad1*. *Dad1* mRNA was increased in RC0.1 cells (R/D = 2.29, 2.12). Dad1, a M_r 12,000 membrane protein, is a subunit of the oligosaccharide transferase complex of the endoplasmic reticulum (60). Although deletion of Dad1 has been found to sensitize cells to apoptosis (61), there is no evidence that overexpression of Dad1 would protect against apoptosis. Because Dad1 is only one of several subunits constituting the antiapoptotic oligosaccharide transferase, the activity of this enzyme complex may not normally be limited by Dad1 availability. Therefore, we are uncertain of the relationship (if any) between the difference in DAD1 mRNA level and the resistance of RC0.1 cells to apoptosis.

Two-Step Model for the Development of Drug Resistance in RC0.1 Cells. The seemingly paradoxical contrary differences between DU145 and RC0.1 mRNA may be explainable by a two-stage model (Fig. 5) for the development of drug resistance. In this model, the first stage alters the expression or activity of one or more gene products (Fig. 5, *box A*) that provide direct resistance to apoptosis. Once this change is in place, genes in upstream pathways (Fig. 5, *box B*) are relieved of constraints imposed by the proapoptotic effects of their over- or underexpression. That is, expression changes that would normally favor selection if they did not also induce apoptosis would become possible without death of the cell. For example, E2F1 and c-Myc stimulate cell cycle progression as well as apoptosis. According to the above hypothesis, once relieved of the proapoptotic impact of these genes, the cells would be free to express the genes at higher levels and thereby achieve a selective advantage in the presence of drug.

In the current study, Fig. 5, *box A,* includes caspases and the Bcl-2 protein family, particularly the proapoptotic member BAD. It also includes some proteins that affect the activity of BAD post-transcriptionally, particularly by way of Akt/PKB. In the current study, Fig. 5, *box B,* includes transcription products governed by the NFκB and Smad transcription factors. Fig. 5, *box A,* corresponds approximately to the right half of Fig. 4*A*; Fig. 5, *box B,* corresponds approximately to the left half.

Fig. 5, *box B,* proteins may enhance the ability of cells to proceed through the cell cycle despite various types of stress and/or to continue proliferating despite relatively high cell densities. Either mechanism could provide a selective advantage in the presence of drug. However, according to the model, this route to increased drug resistance is prevented as long as changes in the expression of Fig. 5, *box B,* proteins would also induce apoptosis. This model for a route to drug resistance is analogous to a possible mechanism for the origin and progression of malignant tumors recently discussed by Hickman (62); malignancy is deterred as long as unfettered proliferation remains linked to apoptosis. When the route to apoptosis is blocked, proliferative mechanisms are free to wreak havoc.

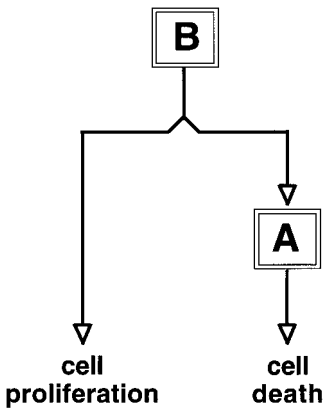

Fig. 5. A hypothetical schematic model ("permissive apoptosis-resistance") for two-stage selection of apoptosis-resistant cells. *Box A* includes proteins that affect apoptosis without major effects on control of cell proliferation. *Box B* includes proteins that affect cell proliferation and also affect apoptosis via genes in *Box A*. *Box A* corresponds approximately to the *right half* of the molecular interaction map in Fig. 4*A*, and *Box B* to the *left half* (see text for details). Growth in the presence of drug selects for cells that are apoptosis-resistant because of changes in the expression of proteins in *Box A*. Once the route to apoptosis via *Box A* has been blocked, cells become free to acquire proliferative advantage by changes in the expression of proteins in *Box B*. This simple model is analogous to that for the role of c-Myc in carcinogenesis when its apoptotic effect has been blocked (68).

Summary and Overview. In the present study, we have used cDNA microarrays in tandem with pharmacological experiments to detect widespread molecular changes in cells and relate them to functional consequences. The overall protocol of the study included: (*a*) Annexin V and APO-BrdUrd flow cytometric assays to measure early and late stages of apoptosis, respectively; (*b*) hybridization of mRNA to cDNA microarrays for gene expression profiling; (*c*) real-time RT-PCR for validation of the microarray data (data not shown); (*d*) formulation of an annotated molecular interaction map for visualization and interpretation of the molecular changes and their consequences; (*e*) statistical analysis of the categories and relationships; (*f*) a first, prospective pharmacological test (using wortmannin) of PI3K involvement in the resistance of RC0.1 to apoptosis; and (*g*) formulation of a two-stage model for the development of resistance.

The study began with the hypothesis that DU145-RC0.1 differences other than the point mutation reported previously in the top1 of RC0.1 were influential in the development of resistance to camptothecin. To explore this hypothesis, we did microarray studies to identify the range of molecules involved and to assess their patterns of change. We first observed that the Akt-PI3K, caspase, and Bcl-2 family portions of the apoptotic machinery showed expression changes in the direction expected for increased resistance to apoptosis in RC0.1. However, the microarray study also yielded the puzzling finding that other sets of molecules associated with apoptosis, principally in the NFκB and TGFβ pathways, seemed to be changing in the contrary direction. Analysis of a molecular interaction map of the relevant genes led us to a two-stage "permissive apoptosis-resistance" hypothesis and model to explain the overall results.

Several obvious limitations of this study should be borne in mind. First, at this point in the development of the technology, mRNA expression profiling is attended by uncertainties, particularly with respect to the distinction among close gene family members. Second, not all of the genes potentially involved in drug resistance were present on the Oncochip array. Absent, for example, were the ATP-binding cassettes, subfamily G (WHITE), member 2 (bcrp), and subfamily C (mrp). Genes for multidrug resistance (63), *mdr1* and *3* genes, were present but not significantly changed (R/D = 1.02 and 1.22, respectively), consistent with prior studies demonstrating that camptothecins are not mdr1 substrates (64). Third, differences in transcript expression may not reflect differences in protein expression. Fourth, functional differences may not be reflected directly at the transcript level. Single nucleotide polymorphisms, chromosomal aberrations, and post-translational modifications may be influential. As in any feasible biological study, we were able to investigate only a subset of the possible influences and secondary effects that may have been functionally important. The incompleteness of even this extensive, multifaceted study indicates the need for high-throughput, quite comprehensive approaches to biological systems, to synergize with work done on a gene-by-gene, factor-by-factor basis (65–67).

With respect to differences at the chromosomal level, we do have some contributory evidence, which will be presented in extenso else-

where.[9] Very briefly: (*a*) in bacterial artificial chromosome array-based comparative genomic hybridization studies done in a collaboration with the laboratory of Joe Gray (UCSF, San Francisco, CA)[10,11] we have observed a statistically highly significant correlation between DNA copy number and the expression levels of genes important in the results of the present study; and (b) routine cytogenetics plus spectral karyotyping showed greatly increased genomic instability in RC0.1 and a ploidy-relative amplification of the antiapoptotic gene *BAD*.

ACKNOWLEDGMENTS

We thank Althea Jackson for editorial assistance in preparation of the manuscript, and Dr. Kimberly Bussey for advice and consultation on cytogenetic issues.

REFERENCES

1. Pommier, Y., Pourquier, P., Urasaki, Y., Wu, J., and Laco, G. Topoisomerase I inhibitors: selectivity and cellular resistance. Drug Resistance Update, *2:* 307–318, 1999.
2. Chen, A. Y., and Liu, L. F. DNA Topoisomerases: essential enzymes and lethal targets. Annu. Rev. Pharmacol. Toxicol., *94:* 194–218, 1994.
3. Beck, W. T., Khelifa, T., Kusumoto, H., Mo, Y. Y., Rodgers, Q., Wolverton, J. S., and Wang, Q. Novel mechanisms of resistance to inhibitors of DNA topoisomerases. Adv. Enzyme Regul., *37:* 17–26, 1997.
4. Nieves-Neira, W., and Pommier, Y. Apoptotic response to camptothecin and 7-hydroxystaurosporine (UCN-01) in the eight human breast cancer cell lines of the NCI anticancer drug screen: multifactorial relationship with topoisomerase I, protein kinase C, bcl-2 and caspase pathways. Int. J. Cancer, *82:* 396–404, 1999.
5. Urasaki, Y., Laco, G., Pourquier, P., Takebayashi, Y., Kohlhagen, G., Gioffre, C., Zhang, H., Chatterjee, D., Pantazis, P., and Pommier, Y. Characterization of a novel topoisomerase I mutation from a camptothecin-resistant human prostate cancer cell line. Cancer Res., *61:* 1964–1969, 2001.
6. Weinstein, I. B. Cancer. Addiction to oncogenes–the Achilles heal of cancer. Science (Wash. DC), *297:* 63–64, 2002.
7. Rasmussen, L. J., Rasmussen, M., Lutzen, A., Bisgaard, H. C., and Singh, K. K. The human cyclin B1 protein modulates sensitivity of DNA mismatch repair deficient prostate cancer cell lines to alkylating agents. Exp. Cell Res., *257:* 127–134, 2000.
8. Chen, Y., Wang, J., Fraig, M. M., Metcalf, J., Turner, W. R., Bissada, N. K., Watson, D. K., and Schweinfest, C. W. Defects of DNA mismatch repair in human prostate cancer. Cancer Res., *61:* 4112–4121, 2001.
9. Costa-Pereira, A. P., and Cotter, T. G. Camptothecin sensitizes androgen-independent prostate cancer cells to anti-Fas-induced apoptosis. Br. J. Cancer, *80:* 371–378, 1999.
10. Tang, D. G., Li, L., Chopra, D. P., and Porter, A. T. Extended survivability of prostate cancer cells in the absence of trophic factors: increased proliferation, evasion of apoptosis, and the role of apoptosis proteins. Cancer Res., *58:* 3466–3479, 1998.
11. Chatterjee, D., Schmitz, I., Krueger, A., Yeung, K., Kirchhoff, S., Krammer, P. H., Peter, M. E., Wyche, J. H., and Pantazis, P. Induction of apoptosis in 9-nitrocamptothecin-treated DU145 human prostate carcinoma cells correlates with de novo synthesis of CD95 and CD95 ligand and down-regulation of c-FLIP(short). Cancer Res., *61:* 7148–7154, 2001.
12. Nimmanapalli, R., Perkins, C. L., Orlando, M., O'Bryan, E., Nguyen, D., and Bhalla, K. N. Pretreatment with paclitaxel enhances apo-2 ligand/tumor necrosis factor-related apoptosis-inducing ligand-induced apoptosis of prostate cancer cells by inducing death receptors 4 and 5 protein levels. Cancer Res., *61:* 759–763, 2001.
13. Chatterjee, D., Wyche, J. H., and Pantazis, P. Induction of apoptosis in malignant and camptothecin-resistant human cells. Ann. N. Y. Acad. Sci., *803:* 143–156, 1996.
14. Zhou, Y., Gwadry, F. G., Reinhold, W. C., Miller, L. D., Smith, L. H., Scherf, U., Liu, E. T., Kohn, K. W., Pommier, Y., and Weinstein, J. N. Transcriptional regulation of mitotic genes by camptothecin-induced DNA damage: Microarray analysis of dose- and time-dependent effects. Cancer Res., *62:* 1688–1695, 2002.
15. Agresti, A. Categorical Data Analysis. John Wiley & Sons, Inc., 1990.
16. Kohn, K. W. Molecular interaction map of the mammalian cell cycle control and DNA repair systems. Mol. Biol. Cell, *10:* 2703–2734, 1999.
17. Tanabe, L., Scherf, U., Smith, L. H., Lee, J. K., Hunter, L., and Weinstein, J. N. MedMiner: an Internet text-mining tool for biomedical information, with application to gene expression profiling. Biotechniques, *27:* 1210–1214, 1216–1217, 1999.
18. Yano, H., Nakanishi, S., Kimura, K., Hanai, N., Saitoh, Y., Fukui, Y., Nonomura, Y., and Matsuda, Y. Inhibition of histamine secretion by wortmannin through the blockade of phosphatidylinositol 3-kinase in RBL-2H3 cells. J. Biol. Chem., *268:* 25846–25856, 1993.
19. Li, X., Marani, M., Mannucci, R., Kinsey, B., Andriani, F., Nicoletti, I., Denner, L., and Marcelli, M. Overexpression of BCL-X(L) underlies the molecular basis for resistance to staurosporine-induced apoptosis in PC-3 cells. Cancer Res., *61:* 1699–1706, 2001.
20. Tafani, M., Minchenko, D. A., Serroni, A., and Farber, J. L. Induction of the mitochondrial permeability transition mediates the killing of HeLa cells by staurosporine. Cancer Res., *61:* 2459–2566, 2001.
21. Jan, M. S., Liu, H. S., and Lin, Y. S. Bad overexpression sensitizes NIH/3T3 cells to undergo apoptosis which involves caspase activation and ERK inactivation. Biochem. Biophys. Res. Commun., *264:* 724–729, 1999.
22. Ding, Z., Yang, X., Pater, A., and Tang, S. C. Resistance to apoptosis is correlated with the reduced caspase-3 activation and enhanced expression of antiapoptotic proteins in human cervical multidrug-resistant cells. Biochem. Biophys. Res. Commun., *270:* 415–420, 2000.
23. Ao, Y., Rohde, L. H., and Naumovski, L. p53-interacting protein 53BP2 inhibits clonogenic survival and sensitizes cells to doxorubicin but not paclitaxel-induced apoptosis. Oncogene, *20:* 2720–2725, 2001.
24. Stupack, D. G., Puente, X. S., Boutsaboualoy, S., Storgard, C. M., and Cheresh, D. A. Apoptosis of adherent cells by recruitment of caspase-8 to unligated integrins. J. Cell Biol., *155:* 459–470, 2001.
25. Danilkovitch-Miagkova, A., Angeloni, D., Skeel, A., Donley, S., Lerman, M., and Leonard, E. J. Integrin-mediated RON growth factor receptor phosphorylation requires tyrosine kinase activity of both the receptor and c-Src. J. Biol. Chem., *275:* 14783–14786, 2000.
26. Danilkovitch-Miagkova, A., and Leonard, E. J. Anti-apoptotic action of macrophage stimulating protein (MSP). Apoptosis, *6:* 183–190, 2001.
27. Sarma, V., Lin, Z., Clark, L., Rust, B. M., Tewari, M., Noelle, R. J., and Dixit, V. M. Activation of the B-cell surface receptor CD40 induces A20, a novel zinc finger protein that inhibits apoptosis. J. Biol. Chem., *270:* 12343–12346, 1995.
28. Chu, Z. L., McKinsey, T. A., Liu, L., Gentry, J. J., Malim, M. H., and Ballard, D. W. Suppression of tumor necrosis factor-induced cell death by inhibitor of apoptosis c-IAP2 is under NF-κB control. Proc. Natl. Acad. Sci. USA, *94:* 10057–10062, 1997.
29. Lee, E. G., Boone, D. L., Chai, S., Libby, S. L., Chien, M., Lodolce, J. P., and Ma, A. Failure to regulate TNF-induced NF-κB and cell death responses in A20-deficient mice. Science (Wash. DC), *289:* 2350–2354, 2000.
30. Nozaki, S., Sledge G. W., Jr., and Nakshatri, H. Repression of GADD153/CHOP by NF-κB: a possible cellular defense against endoplasmic reticulum stress-induced cell death. Oncogene, *20:* 2178–2185, 2001.
31. McCullough, K. D., Martindale, J. L., Klotz, L. O., Aw, T. Y., and Holbrook, N. J. Gadd153 sensitizes cells to endoplasmic reticulum stress by down-regulating Bcl2 and perturbing the cellular redox state. Mol. Cell. Biol., *21:* 1249–1259, 2001.
32. Micheau, O., Lens, S., Gaide, O., Alevizopoulos, K., and Tschopp, J. NF-κB signals induce the expression of c-FLIP. Mol. Cell. Biol., *21:* 5299–5305, 2001.
33. Chapman, N. R., and Perkins, N. D. Inhibition of the RelA(p65) NF-κB subunit by Egr-1. J. Biol. Chem., *275:* 4719–4725, 2000.
34. Massague, J., Blain, S. W., and Lo, R. S. TGFβ signaling in growth control, cancer, and heritable disorders. Cell, *103:* 295–309, 2000.
35. Das, A., Chendil, D., Dey, S., Mohiuddin, M., Mohiuddin, M., Milbrandt, J., Rangnekar, V. M., and Ahmed, M. M. Ionizing radiation down-regulates p53 protein in primary Egr-1−/− mouse embryonic fibroblast cells causing enhanced resistance to apoptosis. J. Biol. Chem., *276:* 3279–3286, 2001.
36. Virolle, T., Adamson, E. D., Baron, V., Birle, D., Mercola, D., Mustelin, T., and de Belle, I. The Egr-1 transcription factor directly activates PTEN during irradiation-induced signalling. Nat. Cell Biol., *3:* 1124–1128, 2001.
37. Uchida, K., Suzuki, H., Ohashi, T., Nitta, K., Yumura, W., and Nihei, H. Involvement of MAP kinase cascades in Smad7 transcriptional regulation. Biochem. Biophys. Res. Commun., *289:* 376–381, 2001.
38. Mazars, A., Lallemand, F., Prunier, C., Marais, J., Ferrand, N., Pessah, M., Cherqui, G., and Atfi, A. Evidence for a role of the JNK cascade in Smad7-mediated apoptosis. J. Biol. Chem., *276:* 36797–36803, 2001.
39. Lallemand, F., Mazars, A., Prunier, C., Bertrand, F., Kornprost, M., Gallea, S., Roman-Roman, S., Cherqui, G., and Atfi, A. Smad7 inhibits the survival nuclear factor κB and potentiates apoptosis in epithelial cells. Oncogene, *20:* 879–884, 2001.
40. Weston, C. R., and Davis, R. J. The JNK signal transduction pathway, Curr. Opin. Genet. Dev., *12:* 14–21, 2002.
41. Potapova, O., Basu, S., Mercola, D., and Holbrook, N. J. Protective role for c-Jun in the cellular response to DNA damage. J. Biol. Chem., *276:* 28546–28553, 2001.
42. Leppa, S., Eriksson, M., Saffrich, R., Ansorge, W., and Bohmann, D. Complex functions of AP-1 transcription factors in differentiation and survival of PC12 cells. Mol. Cell. Biol., *21:* 4369–4378, 2001.
43. Lee, L. F., Li, G., Templeton, D. J., and Ting, J. P. Paclitaxel (Taxol)-induced gene expression and cell death are both mediated by the activation of c-Jun NH2-terminal kinase (JNK/SAPK). J. Biol. Chem., *273:* 28253–28260, 1998.
44. Blattner, C., Kannouche, P., Litfin, M., Bender, K., Rahmsdorf, H. J., Angulo, J. F., and Herrlich, P. UV-Induced stabilization of c-fos and other short-lived mRNAs. Mol. Cell. Biol., *20:* 3616–3625, 2000.
45. Perlman, R., Schiemann, W. P., Brooks, M. W., Lodish, H. F., and Weinberg, R. A. TGF-β-induced apoptosis is mediated by the adapter protein Daxx that facilitates JNK activation. Nat. Cell Biol., *3:* 708–714, 2001.
46. Lin, D. Y., and Shih, H. M. Essential role of the 58-kDa microspherule protein in the modulation of Daxx-dependent transcriptional repression as revealed by nucleolar sequestration. J. Biol. Chem., *277:* 25446–25456, 2002.
47. Fleischmann, A., Hafezi, F., Elliott, C., Reme, C. E., Ruther, U., and Wagner, E. F. Fra-1 replaces c-Fos-dependent functions in mice. Genes Dev., *14:* 2695–2700, 2000.

[9] Reinhold *et al.*, manuscript in preparation.

[10] K. Chin, W-L. Kuo, W. C. Reinhold, J. Fridlyand, A. Jain, K. J. Bussey, J. N. Weinstein, J. W. Gray. Genome profiling of NCI60 cell lines using array CGH, manuscripts in preparation.

[11] K. Bussey, K. Chin, W. C. Reinhold, S. Lababidi, F. Gwadry, S. Nishizuka, Ajay, G. Tonon, A. Roschke, K. Stover, I. Kirsch, D. A. Scudiero, J. W. Gray, J. N. Weinstein. Correlation array CGH with gene expression and drug sensitivity in the NCI60 cell line panel, manuscripts in preparation.

48. Leone, G., Sears, R., Huang, E., Rempel, R., Nuckolls, F., Park, C. H., Giangrande, P., Wu, L., Saavedra, H. I., Field, S. J., Thompson, M. A., Yang, H., Fujiwara, Y., Greenberg, M. E., Orkin, S., Smith, C., and Nevins, J. R. Myc requires distinct E2F activities to induce S phase and apoptosis. Mol. Cell, *8:* 105–113, 2001.
49. Yagi, K., Furuhashi, M., Aoki, H., Goto, D., Kuwano, H., Sugamura, K., Miyazono, K., and Kato, M. c-myc is a downstream target of the Smad pathway. J. Biol. Chem., *277:* 854–861, 2002.
50. Eischen, C. M., Packham, G., Nip, J., Fee, B. E., Hiebert, S. W., Zambetti, G. P., and Cleveland, J. L. Bcl-2 is an apoptotic target suppressed by both c-Myc and E2F-1. Oncogene, *20:* 6983–6993, 2001.
51. Soucie, E. L., Annis, M. G., Sedivy, J., Filmus, J., Leber, B., Andrews, D. W., and Penn, L. Z. Myc potentiates apoptosis by stimulating Bax activity at the mitochondria. Mol. Cell. Biol., *21:* 4725–4736, 2001.
52. Goto, S., Ihara, Y., Urata, Y., Izumi, S., Abe, K., Koji, T., and Kondo, T. Doxorubicin-induced DNA intercalation and scavenging by nuclear glutathione S-transferase π. FASEB J., *15:* 2702–2714, 2001.
53. Adler, V., Yin, Z., Fuchs, S. Y., Benezra, M., Rosario, L., Tew, K. D., Pincus, M. R., Sardana, M., Henderson, C. J., Wolf, C. R., Davis, R. J., and Ronai, Z. Regulation of JNK signaling by GSTp. EMBO J., *18:* 1321–1334, 1999.
54. Strange, R. C., Spiteri, M. A., Ramachandran, S., and Fryer, A. A. Glutathione-S-transferase family of enzymes. Mutat. Res., *482:* 21–26, 2001.
55. Borde-Chiche, P., Diederich, M., Morceau, F., Wellman, M., and Dicato, M. Phorbol ester responsiveness of the glutathione S-transferase P1 gene promoter involves an inducible c-jun binding in human K562 leukemia cells. Leuk. Res., *25:* 241–247, 2001.
56. Young, M. R., Nair, R., Bucheimer, N., Tulsian, P., Brown, N., Chapp, C., Hsu, T. C., and Colburn, N. H. Transactivation of Fra-1 and consequent activation of AP-1 occur extracellular signal-regulated kinase dependently. Mol. Cell. Biol., *22:* 587–598, 2002.
57. Nelson, W. G., De Marzo, A. M., Deweese, T. L., Lin, X., Brooks, J. D., Putzi, M. J., Nelson, C. P., Groopman, J. D., and Kensler, T. W. Preneoplastic prostate lesions: an opportunity for prostate cancer prevention. Ann. N. Y. Acad. Sci., *952:* 135–144, 2001.
58. Song, J. Z., Stirzaker, C., Harrison, J., Melki, J. R., and Clark, S. J. Hypermethylation trigger of the glutathione-S-transferase gene (GSTP1) in prostate cancer cells. Oncogene, *21:* 1048–1061, 2002.
59. Lin, X., Asgari, K., Putzi, M. J., Gage, W. R., Yu, X., Cornblatt, B. S., Kumar, A., Piantadosi, S., DeWeese, T. L., De Marzo, A. M., and Nelson, W. G. Reversal of GSTP1 CpG island hypermethylation and reactivation of pi-class glutathione S-transferase (GSTP1) expression in human prostate cancer cells by treatment with procainamide. Cancer Res., *61:* 8611–8616, 2001.
60. Sanjay, A., Fu, J., and Kreibich, G. DAD1 is required for the function and the structural integrity of the oligosaccharyltransferase complex. J. Biol. Chem., *273:* 26094–26099, 1998.
61. Yoshimi, M., Sekiguchi, T., Hara, N., and Nishimoto, T. Inhibition of N-linked glycosylation causes apoptosis in hamster BHK21 cells. Biochem. Biophys. Res. Commun., *276:* 965–969, 2000.
62. Hickman, J. A. Apoptosis and tumourigenesis. Curr. Opin. Genet. Dev., *12:* 67–72, 2002.
63. Kartner, N., Riordan, J. R., and Ling, V. Cell surface P-glycoprotein associated with multidrug resistance in mammalian cell lines. Science (Wash. DC) *221:* 1285–1288, 1983.
64. Hoki, Y., Fujimori, A., and Pommier, Y. Differential cytotoxcity of clinically important camptothecin derivatives in P-glycoprotein-overexpressing cell lines. Cancer Chemother. Pharmacol., *40:* 433–438, 1997.
65. Weinstein, J. N., Myers, T. G., O'Connor, P. M., Friend, S. H., Fornace, A. J., Jr., Kohn, K. W., Fojo, T., Bates, S. E., Rubinstein, L. V., Anderson, N. L., Buolamwini, J. K., van Osdol, W. W., Monks, A. P., Scudiero, D. A., Sausville, E. A., Zaharevitz, D. W., Bunow, B., Viswanadhan, V. N., Johnson, G. S., Wittes, R. E., and Paull, K. D. An information-intensive approach to the molecular pharmacology of cancer. Science (Wash. DC), *275:* 343–349, 1997.
66. Weinstein, J. N. Fishing expeditions. Science (Wash. DC), *282:* 627, 1998.
67. Weinstein, J. N. 'Omic' and hypothesis-driven research in the molecular pharmacology of cancer. Curr. Opin. Pharmacol., *2:* 361–365, 2002.
68. Luscher, B. Function and regulation of the transcription factors of the Myc/Max/Mad network. Gene, *277:* 1–14, 2001.